Low Temperature Physics/Fizika Nizkikh Temperatur, 2012, v. 38, No. 7, pp. 801–807

Magnetoelastic coupling and possibility of spintronic electromagnetomechanical effects

Helen V. Gomonay[1,2], Svitlana V. Kondovych[1], and Vadim M. Loktev[1,2]

[1]*National Technical University of Ukraine "KPI", 37 Peremogy Ave., Kyiv 03056, Ukraine*
E-mail: malyshen@ukrpack.net
vloktev@bitp.kiev.ua

[2]*Bogolyubov Institute for Theoretical Physics National Academy of Sciences of Ukraine*
14-b Metrologichna Str., Kyiv 03680, Ukraine

Received February 21, 2012

Nanoelectromagnetomechanical systems (NEMMS) open up a new path for the development of high speed autonomous nanoresonators and signal generators that could be used as actuators, for information processing, as elements of quantum computers etc. Those NEMMS that include ferromagnetic layers could be controlled by the electric current due to effects related with spin transfer. In the present paper we discuss another situation when the current-controlled behavior of nanorod that includes an antiferro- (instead of one of ferro-) magnetic layer. We argue that in this case ac spin-polarized current can also induce resonant coupled magnetomechanical oscillations and produce an oscillating magnetization of antiferromagnetic (AFM) layer. These effects are caused by i) spin-transfer torque exerted to AFM at the interface with nonmagnetic spacer and by ii) the effective magnetic field produced by the spin-polarized free electrons due to *sd*-exchange. The described nanorod with an AFM layer can find an application in magnetometry and as a current-controlled high-frequency mechanical oscillator.

PACS: **85.75.–d** Magnetoelectronics; spintronics: devices exploiting spin polarized transport or integrated magnetic fields;
75.50.Ee Antiferromagnetics;
75.47.–m Magnetotransport phenomena; materials for magnetotransport;
75.47.De Giant magnetoresistance.

Keywords: antiferromagnetic layer, electromagnetomechanical effects, spin-polarized free electrons.

1. Introduction

Nanoelectromagnetomechanical systems (NEMMS) that convert electromagnetic energy into mechanical motion and *vice versa* are now of great interest for several reasons. First of all, NEMMS themselves give yet another manifestation of the coupling between magnetic and mechanical degrees of freedom. Up to now magnetomechanical interactions were the most completely studied for the systems with no electric current (we are talking about the orientational phase transitions, see, e.g. [1], the coupled magnon-phonon modes [2], formation of a magnetoelastic gap [3] etc.). In these cases one can speak about thermodynamic equilibrium and describe the system with the time-independent equations. At the same time in recent years investigations in physics of magnetic phenomena have moved to a new field of spintronics, where not just the current, but the *spin-polarized* electrical current is a critical component that forms the magnetic properties of — mainly metallic — systems.

On the other hand, recently increased attention to NEMMS is also related with their potential applications. In particular, because of small geometrical size, the fundamental mechanical modes of NEMMS fall into GHz range and corresponding devices could be used as high-frequency actuators and transducers of mechanical motion [4] (see also [5] and references therein). Besides, at low temperatures (much smaller than the energy of fundamental mode) NEMMS show quantized mechanical behavior and thus could be used for the quantum measurements and quantum information processing [6–9]. At last, due to high sensitivity to the external fields, including electric, magnetic and surface stresses, the NEMMS could be used as the effective tools for biological imaging [5], magnetometry [10,11], for the measurement of magnetoelastic properties and magnetic anisotropy of the materials [12] etc.

An effective way to induce nanomechanical oscillations is based on the spin-related phenomena, in particular, on spin transferred torque (STT) predicted by Berger [13] and Slonczewski [14,15]. Flip of the free electron spin at the interfaces between the layers with different magnetic properties is related with the change of the angular momentum and for nanosize objects (like NEMMS) can result in the noticeable rotation, torsion or bending of the sample.

Up to dates, combination of nanomechanics and spintronics is implemented in the devices that include ferromangetic (FM) and nonmagnetic (NM) metallic layers. In a nanowire with an only FM/NM interface the FM layer serves as a polarizer for an electric current, and spin flip processes at the FM/NM interface produce a mechanical torque in the sample [16–19]. Another modification of NEMMS (see [20–22]) is analogous to spin-valves and includes at least two FM layers — one is a polarizer and the magnetization of the other is rotated by STT. Oscillations of magnetization, in turn, induce the mechanical movement, due to the presence of spin-lattice coupling.

In the present paper we propose the NEMMS which includes at least one antiferromagnetic (AFM) layer (see Fig. 1) that could be set into motion by spin-polarized current. Our idea is based on the following facts: i) theoretical predictions [23–25] and experimental evidence [26–30] of STT effects in AFMs; ii) strong (compared to FM) spin-lattice coupling in AFM that reveals itself, e.g., in the pronounced magnetoelastic effects like an energy gap for AFMR frequency [3] and shape-induced magnetic anisotropy [31,32]. In the framework of hydrodynamic-like approach we analyze the coupled magnetomechanical dynamics of nanorod consisting of FM, NM and AFM layers and calculate eigen frequencies and current-induced mechanical and magnetic responses of the system. We show that dissipative and nondissipative components of spin-polarized ac current contribute differently to magnetomechanical motion and thus could be separated experimentally. The proposed device can be also used as a current-driven nanoresonator that produces no magnetic field.

The paper is devoted to the 80-th anniversary of the prominent Ukrainian experimentalist Prof. V.V. Eremenko whose contribution into the field of magnetoelasticity is remarkable and is world-wide recognized.

2. Model

Let us consider the NEMMS that demonstrates the torsional mechanical oscillations, e.g., doubly clamped nanorod (Fig. 1,*a*). In general case, torsional dynamics can be viewed as inhomogeneous (space-dependent) rotation of the crystal lattice with respect to some reference state. On the other hand, the magnetics with the strong enough exchange coupling between the magnetic sublattices have another rotational degrees of freedom, namely, those related with the solid-like rotation of the magnetic sublattices

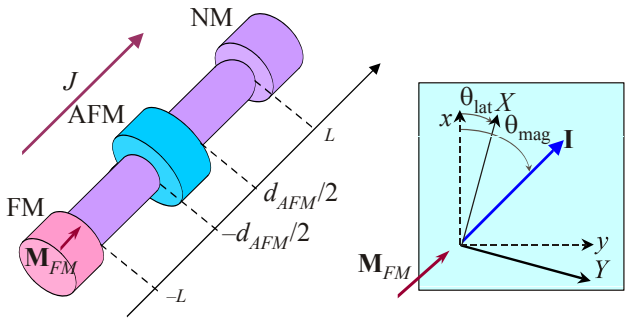

Fig. 1. (Color online) Nanotorsional oscillator. Nanorod made of NM metal with thin AFM section is mechanically clamped between the FM and NM leads (*a*). The current J that flows from FM to NM lead is polarized in $\mathbf{M}_{FM} \parallel Z$ direction and gives rise to the torques twisting the AFM vector $\mathbf{l}$ in the middle section (*b*). Due to magnetic anisotropy, rotation of the magnetic moments through the angle $\theta_{\rm mag}$ induces rotation of the crystal lattice through the angle $\theta_{\rm lat}$. Axes x, y denote the reference frame, while X, Y show the instantaneous orientation of the rotated crystal axes.

[33]. Lattice and magnetic rotations could be coupled due to, e.g., magnetic anisotropy, magnetoelastic or/and shape effects. Thus, any spin torque transferred to the magnetic layer will induce twisting of the crystal lattice and vise versa, any mechanical torque will induce rotations/oscillations of the magnetic subsystem.

In what follows we consider a heterostructure that includes a thin (thickness d_{AFM}) metallic AFM layer inserted just in the middle between two metallic NM rods (each of the length $L \gg d_{AFM}$). Spin-polarized electric current J flowing through this system exerts spin torque to AFM layer due to spin-flip processes at the NM/AFM interface. Thus, the magnetic subsystem serves as a source of the magnetic and, as a result, the mechanical torque for the whole system.

The optimal geometry of the magnetic (FM, or polarizer, and AFM, or "rotator") layers can be predicted from general principles. Curren-induced STT is parallel to the FM magnetization, $\mathbf{M}_{FM}$, so, $\mathbf{M}_{FM}$ should be parallel to the axis of nanorod. On the other hand, the most effective energy transfer between the magnetic and crystal lattices occurs for the modes with the same symmetry. So, an optimal orientation of the magnetic vectors should allow transversal (with respect to nanorod axis) oscillations with the minimal possible frequency.

It should be noted that spin-polarized current acts on AFM layer in three ways. First, STT that is proportional to the spin flux transferred to the magnetic layer and is related with dissipative processes. Second, spin current produces the effective magnetic field $\mathbf{H}_{sd} \propto J\mathbf{M}_{FM}$ parallel to the spin polarization. Corresponding torque that acts on AFM vector is nondissipative (adiabatic). Third, the current itself generates an Oersted field which direction and

value within an AFM layer depends upon the geometry of the system. The last contribution is supposed to produce a negligible effect on AFM dynamics and will be disregarded in the following consideration*. The value of the effective field $\mathbf{H}_{sd}$ depends upon the exchange coupling between free and localized spins (so called *sd*-exchange) and thus can be noticeable, especially in the case of ac current, as will be shown below.

Coupled rotational dynamics of the magnetic and crystal lattices can be described phenomenologically in the framework of continuius approach in terms of the Gibbs' vectors $\varphi_\alpha = \tan(\theta_\alpha/2)\mathbf{e}_\alpha$ that parametrize solid-like rotation of the crystal lattice ($\alpha \Rightarrow \text{lat}$) and magnetic subsystem ($\alpha \Rightarrow \text{mag}$) around an instantaneous rotation axis $\mathbf{e}_\alpha$ through the angle θ_α. Vectors $\varphi_\alpha(\mathbf{r},t)$ are the field variables that define the state of the crystal and magnetic lattices at a moment t in a point $\mathbf{r}$. In the simplest case under consideration (thin nanorod) the rotation axis coinsides with the rod axis, so $\mathbf{e}_{\text{lat}} \parallel \mathbf{e}_{\text{mag}} \parallel Z$.

Time, $\dot{\theta}_\alpha$, and space, $\theta'_\alpha \equiv \nabla_z\theta_\alpha$, derivatives of thus introduced generalized coordinates θ_{lat} and θ_{mag} generate the rotation frequencies and vorticities, correspondingly**.

According to Ref. 33, the rotating magnetic frame produces the dynamic contribution into macroscopic magnetization, M_{AFM}, of AFM. Thus, with account of the effective magnetic field $\mathbf{H}_{sd} \parallel Z$ the magnetization of AFM layer is parallel to the nanorod axis Z and its value is expressed as

$$M_{AFM} = \frac{\chi}{\gamma}(\dot{\theta}_{\text{mag}} + \gamma H_{sd})S_{AFM} = \frac{\chi}{\gamma}(\dot{\theta}_{\text{mag}} + \gamma\beta_{\text{ad}} j)S_{AFM}, \tag{1}$$

where S_{AFM} is the nanorod crossection area within AFM layer, χ is magnetic susceptibility, γ is gyromagnetic ratio. The last expression in (1) includes the material adiabatic (see below) constant β_{ad} that defines the relation between the effective field $H_{sd} = \beta_{\text{ad}} j$ and the the current density $j = J/S_{AFM}$ ***. As follows from definition of the effective field $\mathbf{H}_{sd}$, β_{ad} is proportional to the constant of *sd*-exchange and to the fraction of free electrons that did not flip their spins at NM/AFM interface. Thus, this constant describes the action of nondissipative (adiabatic) component of spin-polarized current, as will be discussed below.

The Lagrange function of the system written from the general symmetry considerations takes a form:

$$\mathcal{L} = \frac{1}{2}\int_{-L}^{L} dz\left[I(z)\,\dot{\theta}_{\text{lat}}^2 - \kappa(\theta'_{\text{lat}})^2 \right] +$$

$$+S_{AFM}\int_{-d_{AFM}/2}^{d_{AFM}/2} dz\left[\frac{\chi}{2\gamma^2}(\dot{\theta}_{\text{mag}} + \gamma\beta_{\text{ad}} j)^2 - U(\theta_{\text{mag}} - \theta_{\text{lat}}) \right]. \tag{2}$$

Here κ is a torsion modulus (rigidity) that can be expressed through the elastic modula and the dimensions of the sample once the geometry is known, $U(\theta_{\text{mag}} - \theta_{\text{lat}})$ is the energy of the magnetic anisotropy which depends upon the relative orientation of the magnetic moments with respect to crystal lattice (see Fig. 1,*b*). A specific (per unit length) moment of inertia of nanorod, $I(z) \equiv \equiv \int \rho_{\text{rod}}(x^2 + y^2)dxdy$, is supposed to be different in NM, $I(z) \equiv I_{NM}$, $d_{AFM}/2 \le |z| \le L$ and in AFM, $I(z) \equiv I_{AFM}$, $|z| \le d_{AFM}/2$ regions, here ρ_{rod} is the nanorod density. In Eq. (2) we have neglected inhomogeneous exchange interactions (terms with θ'_{mag}) that are vanishingly small for a thin (below the characteristic domain wall thickness) AFM layer. We also assume that κ is constant along the rod, generalization for a more complicated case is straightforward.

Dissipative phenomena within an AFM layer that arise from the STT and internal damping are described with the help of generalized potential (or Rayleigh dissipation function) [36] as follows:

$$\mathcal{R}_{AFM} = S_{AFM}\int_{-d_{AFM}/2}^{d_{AFM}/2} dz\left(\chi\frac{\gamma_{AFM}}{\gamma^2}\dot{\theta}_{\text{mag}}^2 - \frac{\beta_{\text{dis}} j}{\gamma}\dot{\theta}_{\text{mag}} \right), \tag{3}$$

where γ_{AFM} is a half-width of AFMR that characterizes the damping. We have also taken into account that the current polarization is parallel to the rod axis, $\mathbf{M}_{FM} \parallel Z$.

The above introduced material constant β_{dis} that describes dissipative component of spin-polarized current needs some special explanation. The value $\beta_{\text{dis}} j$ is equal to spin-flux that is transferred to the unit volume of AFM layer due to spin-flip scattering of the conduction electrons at NM/AFM interface. Thus, two constants, β_{ad} and β_{dis}, though having different physical dimensions, are in a certain sense complementary: the greater is one, the smaller is other.

* According to Refs. 34 and 35 typical value of current-induced Oersted field is 1 kOe. For FM materials with characteristic fields of reorientation 0.1–1 kOe the effect of Oersted field can be significant. However, in AFMs with strong exchange coupling and high Néel temperature (FeMn, IrMn, NiO) the typical value of spin-flop field is higher and falls into 1–10 kOe range. Thus, the effect of the Oersted field can be neglected, at least in the first approximation.

** In general case, frequency is a vector and vorticity is a second rank tensor.

*** Stricktly speaking, current density j is defined by the effective (Sharvin) crossection which in the case of inhomogeneous rod can differ from S_{AFM}.

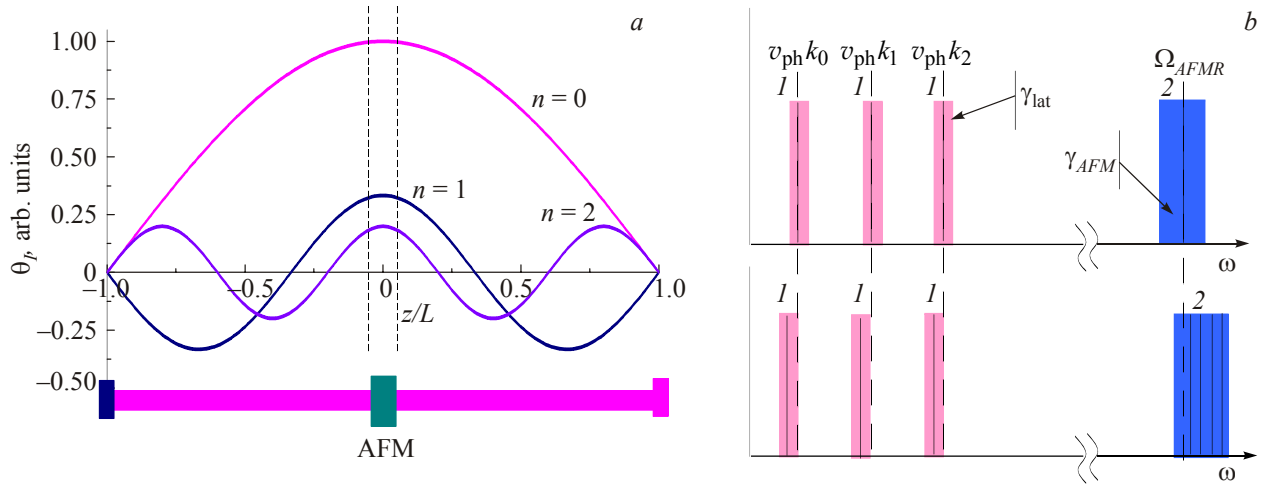

Fig. 2. (Color online) Torsional modes and spectrum of AFM-based nanorod. Low-frequency torsional modes, $\omega = v_{ph}k_n$, $n = 0,1,2$ induced by STT. Relative amplitude of torsional angle, $\theta_{lat}(z)$, is frequency dependent. Low panel schematically shows the position of AFM layer (the thickness $t_{AFM} = 0.02L$ is slightly exaggerated) (*a*). Spectrum of eigen modes (schematically). In the absence of coupling (upper panel) the mechanical modes though smeared (half-width γ_{lat}) are well separated due to the rather high value of quality factor Q_{lat}. The magnetic modes ($\omega = \Omega_{AFMR}$) are degenerated and have a pronounced width (γ_{AFM}). Magnetomechanical coupling (lower panel) results in the (*1*) ("red" online) shift of the mechanical modes and small (*2*) ("blue" online) shift of the magnetic modes (shown by solid vertical lines). While the shifted mechanical modes are still well distinguishable, the spectrum of the shifted magnetic modes falls completely into the line width (*b*).

Damping of the mechanical oscillations are accounted by the corresponding Rayleigh function with the damping constant γ_{lat}:

$$\mathcal{R}_{lat} = \frac{1}{2}\int_{-L}^{L} dz\, I(z)\gamma_{lat}\dot{\theta}_{lat}^2. \qquad (4)$$

Functions (2), (3) and (4) together with the boundary conditions $\theta_{lat}(\pm L) = 0$ (doubly clamped rod) generate the system of dynamic equations for the angles θ_{lat}, θ_{mag} that unambiguously describes the nanorod state. Oscillatory behavior of a system implies small deflections of $\theta_{lat}, \theta_{mag}$ from equilibrium zero values. To this end, magnetic anisotropy can be approximated as $U(\theta_{mag} - \theta_{lat}) \approx \approx \chi\Omega_{AFMR}^2(\theta_{mag} - \theta_{lat})^2/(2\gamma^2)$, where Ω_{AFMR} is AFMR frequency of the mode that corresponds to homogeneous* (within AFM layer) rotation of the magnetic moments around *Z*-axis. It should be stressed that the constant of magnetic anisotropy, $K_{AFM} \equiv \chi\Omega_{AFMR}^2/\gamma^2$, is defined by spin-orbit or dipole interactions and thus includes contribution of magnetoelastic nature.

3. Coupled magnetomechanical dynamics

Let us consider small oscillations induced by ac current $j = j_0 \cos\omega t$. Corresponding equations for the space dependent functions $\theta_{lat}(z)$ and $\theta_{mag}(z)$ in neglection of damping could be reduced to a form:

$$\kappa\frac{d^2\theta_{lat}}{dz^2} + \omega^2\left[I(z) + \frac{S_{AFM}\Theta(z)\chi\Omega_{AFMR}^2}{\gamma^2(\Omega_{AFMR}^2 - \omega^2)}\right]\theta_{lat} =$$

$$= -S_{AFM}\Theta(z)\frac{(\beta_{dis} - i\chi\beta_{ad}\omega)\Omega_{AFMR}^2}{\gamma(\Omega_{AFMR}^2 - \omega^2)}j_0,$$

$$\theta_{mag} = \left[\frac{\Omega_{AFMR}^2\theta_{lat}}{\Omega_{AFMR}^2 - \omega^2} + \frac{\gamma(\beta_{dis} - i\chi\beta_{ad}\omega)}{\chi(\Omega_{AFMR}^2 - \omega^2)}j_0\right]\Theta(z), \quad (5)$$

where form-function $\Theta(z) = 1$ inside the AFM layer ($|z| \le d_{AFM}/2$) and vanishes outside it ($|z| \ge d_{AFM}/2$).

Analysis of Eqs. (5) shows that the spin-polarized current produces a mechanical torque (r.h.s. of the first equation) and thus is a motive force for torsional oscillations. The value of the torque is proportional to the magnetic anisotropy constant $K_{AFM} \propto \Omega_{AFMR}^2$ and the thickness of AFM layer (factor $\Theta(z)$) and can increase greatly in the vicinity of AFMR ($\omega \to \Omega_{AFMR}$). Physical interpretation of this fact is quite obvious: mechanical torque occurs due to spin-lattice coupling within AFM layer and should be proportional to its thickness and coupling constant, the current acts directly on the magnetic subsystem and indirectly on the mechanical one, thus the largest effect should be observed at AFMR frequency.

* As it was already mentioned above, we consider only long-wave motions of AFM subsystem, so-called macrospin approximation.

3.1. Oscillation modes and spectrum

The rod under consideration has two types of the torsion eigen modes, symmetric ($\theta_{\rm lat}(z) = \theta_{\rm lat}(-z)$) and antisymmetric ($\theta_{\rm lat}(z) = -\theta_{\rm lat}(-z)$) with respect to space inversion. From Eqs. (5) it follows that in the present geometry the spin-polarized current can excite only symmetric modes that show maximum deflection $\theta_{\rm lat}$ within an AFM layer ($z \approx 0$).

In the first approximation (taking into account that $d_{AFM} / L \ll 1$) the symmetric modes (see Fig. 2,*a*) could be represented as

$$\theta_{\rm lat}^{(n)}(z,t) = \theta_{\rm lat}^{(n)}(0) e^{i\omega^{(n)}t} \cos k_n z, \qquad (6)$$

$$\theta_{\rm mag}^{(n)}(z,t) = \frac{\Omega_{AFMR}^2 \Theta(z)}{\Omega_{AFMR}^2 - \omega^2} \theta_{\rm lat}^{(n)}(0) e^{i\omega^{(n)}t},$$

were the allowed wave vector $k_n = \pi(2n+1)/(2L)$ is calculated from the boundary conditions. Corresponding eigen frequencies $\omega^{(n)}$ calculated from Eqs. (5) are the following:

$$\omega_{\pm}^{(n)} = \frac{1}{\sqrt{2}} \left\{ \Omega_{AFMR}^2 + (1+\lambda_n) v_{\rm ph}^2 k_n^2 \pm \right.$$

$$\left. \pm \left[(\Omega_{AFMR}^2 - (1+\lambda_n) v_{\rm ph}^2 k_n^2)^2 + 4\lambda_n v_{\rm ph}^2 k_n^2 \Omega_{AFMR}^2 \right]^{1/2} \right\}^{1/2}, \qquad (7)$$

where $v_{\rm ph} = (\kappa/\bar{I})^{1/2}$ is the phonon velocity and $\bar{I} \equiv \equiv (1/2L)\int_{-L}^{L} I(z)dz$ is the averaged moment of inertia. Following the notions of Ref. 20, we have introduced in Eq. (7) the coupling coefficient

$$\lambda_n \equiv \frac{K_{AFM} V_{AFM}}{2L\bar{I} v_{\rm ph}^2 k_n^2} \qquad (8)$$

which is proportional to the magnetic anisotropy of the whole AFM layer (with the volume $V_{AFM} \equiv d_{AFM} S_{AFM}$). Expression (7) for eigen frequencies is analogous to one obtained in Ref. 20 for a nanorod with the FM layer.

The expression (7) confirms quite obvious conclusion that the spectrum of nanorod consists of two branches — high-frequency quasimagnetic, $\omega_{+}^{(n)}$, and low-frequency quasimechanical (torsional), $\omega_{-}^{(n)}$. In the limit $\lambda_n \to 0$ the quasimagnetic frequency $\omega_{+}^{(n)} \to \Omega_{AFMR}$ and quasimechanical one $\omega_{-}^{(n)} \to v_{\rm ph} k_n$.

Further analysis of current-induced dynamics can be simplified due to specification of "small" and "large" quantities. The frequency of the torsional fundamental, "zero", mode for a nanosized rod ($L \propto 30$–100 nm, $v_{\rm ph} \propto 5 \cdot 10^3$ m/s) is $v_{\rm ph} k_0 \propto 10 \div 100$ GHz. Characteristic AFMR frequency for a bulk sample of a typical AFM with high Néel temperature (FeMn, IrMn, NiO) is noticeably greater, $\nu_{AFMR} \equiv \Omega_{AFMR}/2\pi \propto 150$–$1000$ GHz*, depending on the mode type [38–40]. So, in contrast to FM, where the fundamental frequency of the mechanical oscillations is close to the FMR frequency [20], for the nanorods with AFM layer $\Omega_{AFMR} \gg v_{\rm ph} k_0$. However, for higher harmonics (with $n \propto 10$–100) the crossing of frequencies ($v_{\rm ph} k_n \propto \Omega_{AFMR}$) is possible.

The coupling constants $\lambda_n < \lambda_{n-1} < \ldots < \lambda_0 \ll 1$. For example, for a typical AFM $Ir_{20}Mn_{80}$ the anisotropy constant $K_{AFM} \propto 10^5$ J/m^3 [37], so, for the $50 \times 50 \times 2$ nm AFM layer $\lambda_0 \propto 10^{-2}$. However, it should be stressed that the constant λ_0 in AFM is substantially larger than for analogous FM layer (e.g., for Fe the value $\lambda_0 \propto 10^{-3}$ [20]), due to the difference in magnetic anisotropy.

The quality factor of the mechanical oscillations, $Q_{\rm lat} = v_{\rm ph} k_0 / (2\gamma_{\rm lat})$, strongly depends upon the surface effects but even in the worst case is as large as 10^3 [10]. The quality factor of the metallic magnetic subsystem, $Q_{\rm mag} = \Omega_{AFMR} / (2\gamma_{AFM})$, is much smaller, e.g., for the metallic FM the quality factor $Q_{\rm mag} \propto 10^2$ [20].

Thus, the spectrum of the mechanical and magnetic excitations (Eq. (7)) for a typical AFM-based nanorod has the following features (see Fig. 2,*b*):

— in the absence of coupling ($\lambda = 0$) the spectrum of the mechanical modes consists of thin ($Q_{\rm lat} \gg 1$) well-separated lines. The spectrum of the magnetic modes is degenerated ($\omega = \Omega_{AFMR}$), corresponding line is rather thick;

— far from the crossing the coupling-induced shift of the frequencies, $\omega_{-}^{(n)} = v_{\rm ph} k_n (1 - \lambda_n v_{\rm ph}^2 k_n^2 / 2\Omega_{AFMR}^2)$, $\omega_{+}^{(n)} = \Omega_{AFMR} (1 + \lambda_n v_{\rm ph}^2 k_n^2 / 2\Omega_{AFMR}^2)$, is vanishingly small. So, "mechanical" modes are still well separated, while the splitting of the "magnetic" modes is below the line width;

— in the vicinity of crossing the splitting of the mechanical and magnetic modes is substantially greater, $\omega_{\pm}^{(n)} = \Omega_{AFMR} (1 \pm \sqrt{\lambda_n}/2)$. Damping processes are defined mainly by the magnetic subsystem, so, corresponding quality factor is close to $Q_{\rm mag}$. Thus, the magnetic and mechanical modes could be resolved providing $\sqrt{\lambda_n} Q_{\rm mag} > 1$.

3.2. Current-induced oscillations

From the properties of oscillation spectrum it follows that current-induced behavior of nanorod is different in the low-frequency ($\omega \ll \Omega_{AFMR}$) and high-frequency ($\omega \propto \Omega_{AFMR}$) ranges. Let us consider them separately.

In the low-frequency range the last term in the l.h.s. of the first of Eqs. (5) is small ($\propto \lambda$) and can be neglected. To this end, torsion angle of mechanical oscillations is expressed as

* For the small samples ν_{AFMR} can be smaller due to the size effects, see, e.g. [37].

$$\theta_{\rm lat}(z;\omega)=\frac{V_{AFM}\,j_0}{\gamma\bar{I}L}\frac{\pi}{4\omega v_{\rm ph}k_0}\times$$

$$\times\frac{(\beta_{\rm dis}-i\chi\beta_{\rm ad}\omega)\sin\left[(L-|z|)\omega/c\right]}{\sqrt{\cos^2(L\omega/c)+(\pi/4Q_{\rm lat})^2\sin^2(L\omega/c)}}\,{\rm e}^{i\phi},\qquad(9)$$

where ϕ is the frequency dependent phase shift with respect to j, in the vicinity of resonance $\phi\to\pi/2$.

It can be easily seen from Eq. (9) that the current-induced torsional oscillations have clearly defined resonance character at $\omega=\omega_{-}^{(n)}\approx v_{\rm ph}k_n$. Space dependence of $\theta_{\rm lat}(z)$ at a given ω (see Fig. 2,*a*) is close to the mechanical eigen modes. The resonant amplitude obtained from Eq. (9) is

$$\theta_{\rm lat}^{(n)}({\rm res})=\frac{Q_{\rm lat}V_{AFM}\,j_0}{\gamma\bar{I}Lv_{\rm ph}^2k_0^2}\left(\frac{i\beta_{\rm dis}}{2n+1}+\chi\beta_{\rm ad}v_{\rm ph}k_0\right)=$$

$$=\frac{2\lambda_0Q_{\rm lat}\gamma j_0}{\Omega_{AFMR}^2\chi}\left(\frac{i\beta_{\rm dis}}{2n+1}+\chi\beta_{\rm ad}v_{\rm ph}k_0\right).\qquad(10)$$

Here the factor i reflects the phase shift of the torsion angle with respect to current.

As seen from Eq. (10), rotation of lattice results from two effects induced by spin-polarized current, namely, dissipative STT ($\propto\beta_{\rm dis}$) and adiabatic effective spin-induced field ($\propto\beta_{\rm ad}$). The first contribution diminishes with the frequency ($\propto n$) growth, while the second one is frequency independent (at least, for $\omega\ll\Omega_{AFMR}$). Moreover, STT-induced term is phase-shifted with respect to current, while adiabatic term is in phase with current. This opens a way to separate these contributions by measuring current dependence of resonant torsional oscillations.

An amplitude of the corresponding magnetic oscillations differs from $\theta_{\rm lat}^{(n)}({\rm res})$ by the factor $(1+2i\lambda_0Q_{\rm lat})$, as seen from the following

$$\theta_{\rm mag}^{(n)}({\rm res})=\frac{\gamma j_0}{\chi\Omega_{AFMR}^2}(1+2i\lambda_0Q_{\rm lat})\left(\frac{\beta_{\rm dis}}{2n+1}-i\chi\beta_{\rm ad}v_{\rm ph}k_0\right).\qquad(11)$$

It also depends upon both dissipative and nondissipative current-induced contributions, however, phase shift with respect to current is much more complicated due to the term with $\lambda_0Q_{\rm lat}$. Time derivative $\dot\theta_{\rm mag}^{(n)}({\rm res})=$ $=iv_{\rm ph}k_n\theta_{\rm mag}^{(n)}({\rm res})$ is proportional to magnetization of AFM layer (see Eq. (1) and thus can be detected experimentally.

In the high-frequency range the magnetic modes with different n are almost degenerated. So, the current induces mechanical,

$$\theta_{\rm lat}({\rm res})=\frac{15Q_{AFM}V_{AFM}\,j_0}{16\gamma\bar{I}L\Omega_{AFMR}^2}\left(i\beta_{\rm dis}+\chi\beta_{\rm ad}\Omega_{AFMR}\right),\qquad(12)$$

and magnetic,

$$\theta_{\rm mag}({\rm res})=-\frac{\gamma Q_{AFM}\,j_0}{\chi\Omega_{AFMR}^2}\left(i\beta_{\rm dis}+\chi\beta_{\rm ad}\Omega_{AFMR}\right)\times$$

$$\times\left(1+\frac{15v_{\rm ph}^2k_0^2}{8\Omega_{AFMR}^2}\lambda_0Q_{AFM}\right)\qquad(13)$$

oscillations with the frequency $\omega\approx\Omega_{AFMR}$.

4. Conclusions

In the present paper we considered new aspect of magnetoelastic interactions and studied magnetomechanical oscillations induced by spin-polarized current for the simplest case of twisting nanorod. Our calculations demonstrate that ac spin-polarized current can excite quasimechanical (torsional) as well as quasimagnetical modes.

It is interesting to note that the ac spin-polarized current affects the AFM layer in the case of strong scattering at NM/AFM interface (due to STT effect) and in the case of weak scattering as well (due to the effective *sd*-exchange field "injected" with free electrons into AFM layer). Ratio between dissipative and nondissipative contribution is proportional to the phase shift between mechanical oscillations and current and thus can be measured experimentally in the low frequency range.

An amplitude of quasimechanical mode depends upon the geometry of the sample (see Eq. (10)) and can be enhanced by diminishing the moment of intertia (e.g., by using carbon nanotubes [41]) and by enlarging AFM volume V_{AFM}. However, if the thickness of AFM layer, d_{AFM}, becomes greater than the free path of spin-polarized electrons, contribution of dissipative (STT) part will be reduced.

The effectiveness of the described electric-through-magnetic-to-mechanical energy conversion can be increased by using nanorod with periodical FM/NM/AFM structure, however this system needs additional treatment and is out of scope of this paper.

In this work we considered torsional oscillations of the effectively one dimensional structure. Analogous results could be obtained for nanobeams that show flexional oscillations.

The authors acknowledge partial financial support from the Special Program for Fundamental Research of the Department of Physics and Astronomy of National Academy of Sciences of Ukraine. The work of H.G. and S.K. was partially supported by the grant from the Ministry of Education and Science of Ukraine.

1. V. Eremenko and V. Sirenko, *Magnetic and Magnetoelastic Properties of Antiferromagnets and Superconductors, Cambridge Scientific Publishers,* England, Cambridge (2007).
2. A. Akhiezer, V. Bar'yakhtar, and S. Peletminskii, *Sov. J. Theor. Exp. Phys.* **35**, 228 (1958).
3. A.S. Borovik-Romanov, E.G. Rudashevskii, E.A. Turov, and V.G. Shavrov, *Phys.-Usp.* **27**, 642 (1984).

4. M. Li, H. Tang, and M. Roukes, *Nature Nanotechnology* **2**, 114 (2007).
5. K. Eom, H.S. Park, D.S. Yoon, and T. Kwon, *Phys. Rep.* **503**, 115 (2011).
6. N. Zhao, D.-L. Zhou, and J.-L. Zhu, *Commun. Theor. Phys.* **50**, 1457 (2008).
7. S. Savel'ev, A.L. Rakhmanov, X. Hu, A. Kasumov, and F. Nori, *Phys. Rev.* **B75**, 165417 (2007).
8. A.N. Cleland and M.R. Geller, *Phys. Rev. Lett.* **93**, 070501 (2004).
9. D.A. Garanin and E.M. Chudnovsky, *ArXiv e-prints 1104.1170* (2011).
10. J.P. Davis, D. Vick, D.C. Fortin, J.A.J. Burgess, W.K. Hiebert, and M.R. Freeman, *Appl. Phys. Lett.* **96**, 072513 (2010).
11. J. Losby, J.A.J. Burgess, C.M.B. Holt, J.N. Westwood, D. Mitlin, W.K. Hiebert, and M.R. Freeman, *J. Appl. Phys*. **108**, 123910 (2010).
12. S.C. Masmanidis, H.X. Tang, E.B. Myers, M. Li, K. de Greve, G. Vermeulen, W. van Roy, and M.L. Roukes, *Phys. Rev. Lett*. **95**, 187206 (2005).
13. L. Berger, *Phys. Rev.* **B54**, 9353 (1996).
14. J.C. Slonczewski, *Phys. Rev.* **B39**, 6995 (1989).
15. J. Slonczewski, *J. Magn. Magn. Mater.* **159**, L1 (1996).
16. P. Fulde and S. Kettemann, *Ann. Phys*. **7**, 214 (1998).
17. P. Mohanty, G. Zolfagharkhani, S. Kettemann, and P. Fulde, *Phys. Rev*. **B70**, 195301 (2004).
18. P. Mohanty, D.A. Harrington, K.L. Ekinci, Y.T. Yang, M.J. Murphy, and M.L. Roukes, *Phys. Rev.* **B66**, 085416 (2002).
19. G. Zolfagharkhani, A. Gaidarzhy, P. Degiovanni, S. Kettemann, P. Fulde, and P. Mohanty, *Nature Nanotechnology* **3**, 720 (2008).
20. A.A. Kovalev, G.E.W. Bauer, and A. Brataas, *J. Appl. Phys. Jpn.* **45**, 3878 (2006).
21. A.A. Kovalev, G.E.W. Bauer, and A. Brataas, *Phys. Rev.* **B75**, 014430 (2007).
22. A.A. Kovalev, L.P. Zarbo, Y. Tserkovnyak, G.E.W. Bauer, and J. Sinova, *Phys. Rev. Lett.* **101**, 036401 (2008).
23. Y. Xu, S. Wang, and K. Xia, *Phys. Rev. Lett.* **100**, 226602 (2008).
24. P.M. Haney and A.H. MacDonald, *Phys. Rev. Lett.* **100**, 196801 (2008).
25. H.V. Gomonay and V.M. Loktev, *Phys. Rev.* **B81**, 144427 (2010).
26. Z. Wei, A. Sharma, A.S. Nunez, P.M. Haney, R.A. Duine, J. Bass, A.H. MacDonald, and M. Tsoi, *Phys. Rev. Lett.* **98**, 116603 (2007).
27. S. Urazhdin and N. Anthony, *Phys. Rev. Lett.* **99**, 046602 (2007).
28. X.-L. Tang, H.-W. Zhang, H. Su, Z.-Y. Zhong, and Y.-L. Jing, *Appl. Phys. Lett.* **91**, 122504 (2007).
29. N.V. Dai, N.C. Thuan, L.V. Hong, N.X. Phuc, Y.P. Lee, S.A. Wolf, and D.N.H. Nam, *Phys. Rev.* **B77**, 132406 (2008).
30. J. Bass, A. Sharma, Z. Wei, and M. Tsoi, *J. Magnetics* **13**, 1 (2008).
31. V. Kalita, A. Lozenko, S. Ryabchenko, and P. Trotsenko, *Fiz. Nizk. Temp.* **31**, 1042 (2005) [*Low Temp. Phys*. **31**, 794 (2005)].
32. H.V. Gomonay and V.M. Loktev, *Phys. Rev.* **B75**, 174439 (2007).
33. A.F. Andreev and V.I. Marchenko, *Phys.-Usp.* **23**, 21 (1980).
34. M.A. Hoefer, T.J. Silva, and M.D. Stiles, *Phys. Rev.* **B77**, 144401 (2008).
35. M.R. Pufall, W.H. Rippard, M. Schneider, and S.E. Russek, *arXiv:cond-mat/0702416*.
36. H.V. Gomonay, R. Kunitsyn, and V.M. Loktev, *Phys. Rev. B* (2012), *in press.*
37. S.K. Mishra, F. Radu, S. Valencia, D. Schmitz, E. Schierle, H.A. Dürr, and W. Eberhardt, *Phys. Rev.* **B81**, 212404 (2010).
38. Y. Endoh, G. Shirane, Y. Ishikawa, and K. Tajima, *Solid State Commun.* **13**, 1179 (1973).
39. J. Nishitani, K. Kozuki, T. Nagashima, and M. Hangyo, *Appl. Phys. Lett*. **96**, 221906 (2010).
40. T. Satoh, S. Cho, R. Iida, T. Shimura, K. Kuroda, H. Ueda, Y. Ueda, B.A. Ivanov, F. Nori, and M. Fiebig, *Phys. Rev. Lett.* **105**, 077402 (2010).
41. P.A. Williams, S.J. Papadakis, A.M. Patel, M.R. Falvo, S. Washburn, and R. Superfine, *Phys. Rev. Lett.* **89**, 255502 (2002).